Assessing reliability of learning Gaussian graphical models from microbial abundances

Francisco Campuzano Jiménez[1]

[1]Bioinformatics Research Centre, Aarhus University

2024-01-18

Table of contents

1 Introduction

Microbial networks are temporary or spatial snapshots of ecosystems, where taxonomic units are displayed as nodes (but also environmental variables) and significant associations as undirected edges (Röttjers and Faust 2018). Microbial taxa associations in situ cannot be assessed by observing interactions, as we typically do for macro ecosystems (Guseva et al. 2022). Therefore, methods based on co-occurrence data from amplicon and metagenomic sequencing and their interpretation are an active and controversial research topic (Blanchet, Cazelles, and Gravel 2020).

Undirected Gaussian graphical models have become increasingly popular in the field of microbial ecology for inferring microbial networks. Among other things, because they are less affected by correlated but indirectly connected taxa[1] than correlation-based methods (Matchado et al. 2021). This project focuses on them and on the reliability of their results. We assessed it under typical conditions of working with environmental samples, which are characterized by a limited number of samples. We compared two methods, SpiecEASI (Kurtz et al. 2015), the most popular approach, and one novel Bayesian alternative based on the BDgraph R package (R. Mohammadi and Wit 2019).

2 Background

Formally, a microbial co-occurrence network is a representation of the conditional dependence structure between microbial abundances. The biological meaning of networks has been qualified as uncertain, and requires careful interpretation. Networks are often highly dense and intricate, which makes its use difficult for exploratory analysis (Faust 2021).

Researchers can, instead, analyze the emergent network properties and link them to biology. Here are some possibilities from the literature that motivate the interest in microbial networks. They can be used to study whether some taxonomic units tend to co-occur with each other more often. Clusters of taxonomic units, hereafter modules, may correspond to taxonomic units that share niche preference (Chaffron et al. 2010). Point summaries such as the modularity[2] can be used to assess the impact of an intervention on community architecture (Lurgi et al. 2019; Faust 2021).

In addition, node centrality measurements, such as the hub score[3], might indicate whether certain taxonomic units have broader niche preferences than others (but do not identify keystone[4] species, as they are often misused) (Guseva et al. 2022). Additional sources of information can be integrated in the analysis, for example, by studying the correlation between phylogenetic and network distances[5] (Morueta-Holme et al. 2016). Microbial co-occurrence networks have a great potential in the field of microbial ecology, which has historically been mostly descriptive (Prosser 2020).

2.1 Gaussian graphical models

The following is a brief conceptualization of Gaussian graphical models we adapted from Uhler (2017). Let $G = (V, E)$ be an undirected graph with nodes $V = \{1, \dots, p\}$ and edges $E \subset \{(i, j) \in V \times V : i < j\}$. In our application context, V is a set of microbial taxonomic units, although it can be extended to

[1] Let us consider three random variables A, B, and C, which correspond to the abundances of the three taxonomic units. We say that A and C are indirectly connected (through B) if $\Pr(A|BC) = \Pr(A|B)$, $\Pr(B|AC) = \Pr(B)$ and $\Pr(C|AB) = \Pr(C|B)$.

[2] It quantifies the extent to which a network can be divided into modules. Formally, $Q = \frac{1}{2m} \sum_{ij} \left(A_{ij} - \gamma \frac{k_i k_j}{2m} \right) \mathbb{1}_{c_i = c_j}$, where m is the number of edges, A is the adjacency matrix, k_x is the degree of node x, and c_x is the cluster of node x (Clauset, Newman, and Moore 2004).

[3] Hub scores are defined for undirected networks as the principal eigenvector of $A^\top A$, where A is the adjacency matrix (Kleinberg 1998a).

[4] "A species whose impact on its community or ecosystem is large, and disproportionately large relative to its abundance" (Power et al. 1996).

[5] The shortest path between two nodes is that with a minimal number of edges.

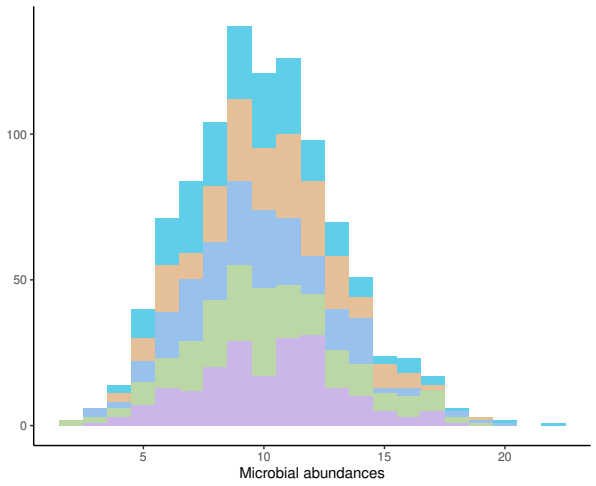

(a)

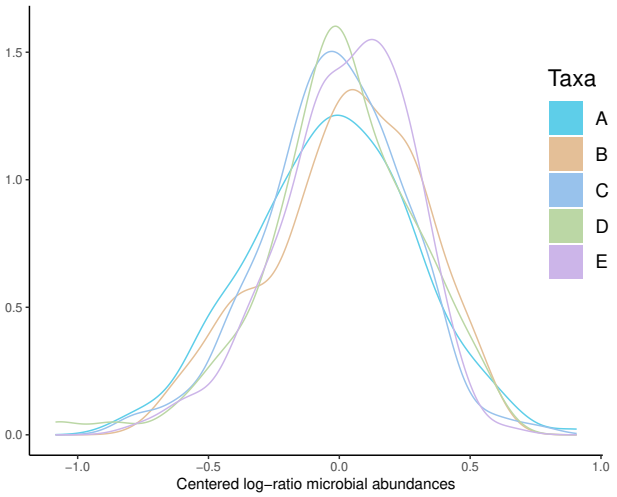

(b)

$$\hat{\Omega}(\lambda = 0.26)$$

$$\begin{bmatrix} & A & B & C & D & E \\ A & 0.85 & 0.00 & 0.00 & 0.11 & 0.19 \\ B & 0.00 & 0.84 & 0.18 & 0.09 & 0.00 \\ C & 0.00 & 0.18 & 0.85 & 0.00 & 0.13 \\ D & 0.11 & 0.09 & 0.00 & 0.82 & 0.00 \\ E & 0.19 & 0.00 & 0.13 & 0.00 & 0.85 \end{bmatrix}$$

(c)

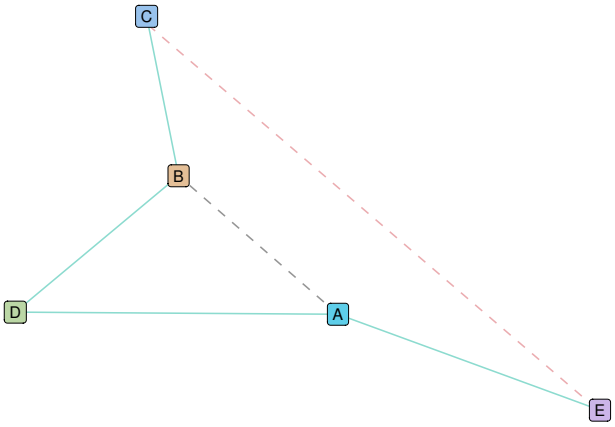

(d)

Figure 1: Inferring a microbial network involves transforming the data and determining the graph structure from a sparse precision matrix estimate. The most popular method for estimating a sparse precision matrix is the graphical lasso estimator. (a) Abundances of five different taxonomic units across 200 samples. (b) Centered log-ratio transformed abundances to address compositionality and the assumption of normality. (c) Graphical lasso estimation of precision matrix ($\lambda = 0.26$). (d) Graph structure that corresponds to the zero-pattern of $\hat{\Omega}(\lambda = 0.26)$. False positive edges are shown in light red, and false negatives in gray.

include environmental factors. We define the edges of the graph such that the absence of edge (i, j) implies conditional independence between the abundances of taxonomic units i and j given all other variables.

We can infer the desired graph G from data by first estimating the inverse of the covariance matrix, known as the precision matrix $\Omega := \Sigma^{-1}$. The precision matrix is useful because, for every matrix element, it is true that $\Omega_{ij} = 0$ if and only if i and j are conditionally independent given the remaining dimensions. We can then unambiguously determine the graph structure from the pattern of zero entries in the precision matrix (see Figure 1c and Figure 1d). Formally, we say that a random variable $X \in \mathbb{R}_p$ follows $G = (V, E)$ if it is distributed as $\mathcal{N}_p(0, \Omega^{-1})$, where Ω is a positive definite matrix of dimensions $p \times p$ such that $\Omega_{ij} = 0$ implies $(i, j) \notin E$. We require that Ω is a positive definite matrix so it is invertible, a well known fact from linear algebra.

Research on inferring microbial networks using graphical models has focused exclusively on estimating sparse Gaussian graphical models. The most popular approach to induce sparsity is imposing a L_1 penalty on the precision matrix. This approach succeeded in the likelihood framework under the name of graphical lasso (Friedman, Hastie, and Tibshirani 2008).

2.2 Data transformation

Unfortunately, microbial abundance data is not normal (see Figure 1a). In the literature, some methods overcome this issue by applying a transformation to the original discrete counts. Even worse, microbial abundance data are highly compositional because of the unequal depth and sampling. To compare abundances between samples the observed counts, $\hat{W} \in \mathbb{N}_{n \times p}$, can be normalized by the total sum of counts per sample.

However, this normalization imposes a sum-to-one constraint, making the relative abundances $X \in \mathbb{R}^+_{n \times p}$ of the different taxonomic units no longer independent. Kurtz et al. (2015) proposed the application of the centered log-ratio transformation (see Equation 1) to the relative abundances, and estimated the Gaussian graphical model from the transformed data $Z \in \mathbb{R}_{n \times p}$ (see Figure 1b). This is the most widely used transformation.

$$Z_{ij} = \log \left(\frac{X_{ij}}{\left[\prod_{m=1}^{p} X_{im}\right]^{\frac{1}{p}}} \right) \tag{1}$$

We denote the per-sample total count sum as $m_i = \sum_{m=1}^{p} W_{i,m}$. The intuition behind the centered log-ratio transformation is that because $\log \frac{W_{i*}}{W_{j*}} = \log \frac{W_{i*}/m_*}{W_{j*}/m_*} = \log \frac{X_{i*}}{X_{j*}}$, the statistical inference performed with the log ratios of relative abundances is equivalent to that performed with the log ratio of unobserved absolute abundances (Kurtz et al. 2015).

SpiecEASI[6] uses the centered-log ratio approach (Kurtz et al. 2015), and so we have done. However, this transformation is not exempt from criticism. Because of the numerical problems with the geometric mean of the samples in Equation 1, SpiecEASI uses pseudo-counts instead of the original values. When data are zero-inflated, the transformed data exhibit a peak corresponding to the spike at zero, which violates the normality assumption and might lead to spurious associations (Ha et al. 2020).

[6] SpiecEASI stands for SParse InversE Covariance Estimation for ecological ASsociation Inference

2.3 Inferring an sparse graph

2.3.1 Likelihood framework

In the likelihood framework, the sparse Gaussian graphical model is usually formulated according to Friedman, Hastie, and Tibshirani (2008).

$$\begin{aligned} \mathcal{L}(\Omega) &= \log|\Omega| - \text{trace}(\hat{\Sigma}\Omega) \\ \hat{\Omega}(\lambda) &= \arg\min_{\Omega \in M^+} (-L(\Omega) + \lambda||\Omega||_1) \end{aligned} \tag{2}$$

where M^+ is the set of positive definite matrices, $\hat{\Sigma}$ is the empirical covariance matrix, and $||\Omega||_1$ is the L_1 norm (the sum of all the absolute values of the matrix). $\mathcal{L}(\Omega)$ is the log-likelihood of the data after maximizing the mean vector μ and ignoring constants. λ is a positive regularization parameter that controls the sparsity of the estimated precision matrix, $\hat{\Omega}(\lambda)$, and consequently, of graph $G(\lambda)$.

Friedman, Hastie, and Tibshirani (2008) proposed an algorithm that efficiently solves the optimization problem shown in Equation 2. Previously, Meinshausen and Bühlmann (2006) suggested that it is sufficient to estimate the pattern of zero elements, rather than the whole matrix to determine the graph. This pattern can be inferred by fitting p lasso regressions and using each variable as the response variable. Let us denote as $\hat{\beta}_a^b$ the a-coefficient of the lasso regression with the b variable as the response for a given value of λ. Their method constrains the estimated graph by excluding all edges (i, j) where either $\hat{\beta}_i^j = 0$ or $\hat{\beta}_j^i = 0$.

The sparsity of the true graph, thus, of the true unknown precision matrix, is unknown. The challenge faced by likelihood-based methods is the selection of an appropriate value of λ. Different criteria may be used, such as selecting λ so it optimizes the Akaike information criterion, the Bayesian information criterion, or the largest within one standard error of the optimal negative likelihood when performing cross-fold validation (or any equivalent rule of thumb) (Liu, Roeder, and Wasserman 2010). However, since the publication of the SpiecEASI method (Kurtz et al. 2015), nearly all microbial co-occurrence network inferences have used the StARS[7] selection method (Liu, Roeder, and Wasserman 2010).

The StARS method is a general procedure that can be applied to any graph-inference method. However, the authors built it on top of the Meinshausen and Bühlmann method. Despite its simplicity, it provides better results in terms of speed, recall and precision than the alternatives (Kurtz et al. 2015). The core idea of StARS is to draw many random overlapping subsamples (without replacement) and apply the Meinshausen and Bühlmann method to each subsample with decreasing values of λ until there is a small but acceptable amount of variability.

They defined the variability in terms of the average total instability of the edges. Specifically, for any chosen λ, they estimate m graphs, one for each m subsample. They calculated the instability of a particular edge (i, j) as the fraction of every possible pair of m graphs that disagree in the presence or absence of an (i, j) edge. Liu, Roeder, and Wasserman (2010) stated that they could estimate a graph containing the true graph with high probability by selecting the largest value of λ (the sparsest graph) for which the average total instability is equal to or more than β. They claimed that this cut-off point β is an interpretable quantity (so they did not simply replace the problem of choosing λ to choose β) and that a reasonable default value is $\beta = 0.05$.

2.3.2 Bayesian framework

Different versions of the graphical lasso estimator have been proposed in the Bayesian framework (Wang 2012; Piironen and Vehtari 2017; Richard Li, McCormick, and Clark 2019; Li, Craig, and Bhadra 2019).

[7] StARS stands for Stability Approach to Regularization Selection.

However, its application to microbial co-occurrence network inference is not entirely satisfactory. Because the lasso prior places no probability of any value of the precision matrix being exactly zero, $\Omega_{ij} = 0$, there is no probability of the event $\Omega_{ij} = 0$ in the posterior either. This means that we require a post hoc heuristic to include or exclude an edge from the inferred sparse graph (which is our desired estimand, not the precision matrix). For example, that all off-diagonal elements are set to zero if the 95% credibility interval contains a zero value (Jongerling, Epskamp, and Williams 2023).

The alternative is to use a family of priors called G-Wishart, which is a discrete and continuous mixture prior distribution. If so, we estimate the joint posterior distribution of the precision matrix and graph, as shown in Equation 3.

$$P(G, \Omega|Z) \propto P(Z|G, \Omega)P(\Omega|G)P(G) \tag{3}$$

$P(Z|G, \Omega)$ corresponds to the likelihood function of a multivariate normal distribution, as in the frequentist graphical lasso. The G-Wishart distribution is a convenient prior choice for the precision matrix, $P(\Omega|G)$, because it is conjugated with this likelihood (Roverato 2002). The G-Wishart distribution of a given graph, $W_G(b, D)$, depends on the number of degrees of freedom $b > 2$ and the matrix $D \in M^+$ which is usually set to be the identity matrix. Note that, in Equation 4, we ensure Ω is a valid precision matrix by multiplying the probability by the indicator variable $\mathbb{1}_{\Omega \in M^+}$ (i.e., setting the probability of any nonpositive definite matrix to zero).

$$P(\Omega|G) \propto |\Omega|^{(b-2)/2} \exp\left\{-\frac{1}{2}\text{trace}(D\Omega)\right\} \mathbb{1}_{\Omega \in M^+} \tag{4}$$

Many priors have been proposed for the graph structure, $P(G)$ (Jones et al. 2005; Carvalho and Scott 2009; A. Mohammadi and Wit 2015). A popular choice depends on a $\theta \in (0, 1)$ parameter that expresses our prior belief in the sparsity of the graph (see Equation 5). The larger the graph size, i.e. the number of edges, denoted by $|E|$, the less likely the graph is. Note that, if $\theta = 0.5$, the distribution corresponds to a uniform distribution over the entire graph space.

$$P(G) \propto \left(\frac{\theta}{1-\theta}\right)^{|E|} \tag{5}$$

To explore the graph space and estimate the model parameters simultaneously, we need a particular type of algorithm, the so-called trans dimensional Markov Chain Monte Carlo (A. Mohammadi and Wit 2015). Unfortunately, the graph space is exponentially large[8] and convergence is complex. A. Mohammadi and Wit (2015) proposed a birth-death MCMC, which works well in practice. Every edge is added or removed according to two independent Poisson birth and death processes. The algorithm is formulated such that the posterior distribution of a graph is proportional to how much time the sampling algorithm remained in a particular graph after a certain amount of iterations.

In contrast to the likelihood method, the estimate we obtain is the full posterior distribution $P(G, \Omega|Z)$. A graph point estimate is usually estimated by Bayesian model averaging. First, the average edge inclusion probability of every possible edge is computed as the fraction of times that edge was found in the sampled graphs. Then, a graph is constructed with all the edges whose probability is greater than a specified threshold.

[8] Specifically, $2^{p(p-1)/2}$ graphs exist.

3 Results

3.1 Simulation of synthetic datasets

We simulated data for 53 graphs from different topology and graph sizes (see Figure 2). First, we simulated a graph and normal multivariate data such that their precision matrix was compatible with it. We then simulated microbial abundances that correlated with the normal multivariate distribution. The abundance of each taxonomic unit was drawn from a negative binomial distribution and unequal depths between the samples. For more details, see the Methods section.

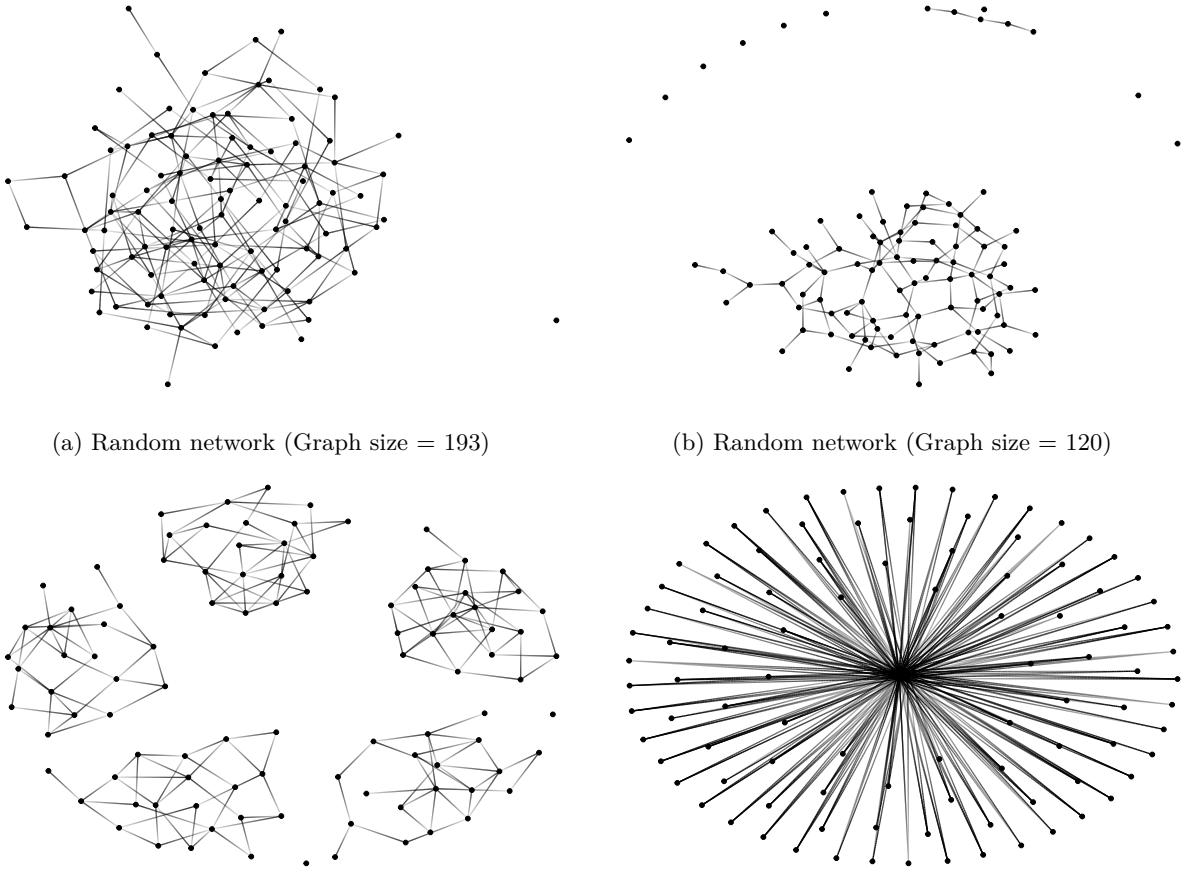

(a) Random network (Graph size = 193)

(b) Random network (Graph size = 120)

(c) Cluster network (Graph size = 184)

(d) Hub network (Graph size = 294)

Figure 2: We analyzed three representative network topologies: random, hub, and cluster. The subfigures show four randomly simulated networks with 100 nodes (taxonomic units) and different numbers of edges (graph size).

3.2 Recovery of microbial networks

We evaluated the recovery of the true graph from datasets of increasing sample size. We analyzed the 53 graphs and their respective data. In addition to microbial counts, to which we applied the centered log-ratio transformation, we evaluated performance when inference was performed with the noiseless normal multivariate data. The latter would correspond to performing the inference as if we had access to the latent random variables.

As mentioned before, we considered two methods: SpiecEASI and its Bayesian alternative with a G-Wishart prior based on BDgraph. More specifically, we assessed the completeness of the optimal graph selected by SpiecEASI when setting $\beta = 0.05$, and of the Bayesian method when predicting the graphs of all the edges

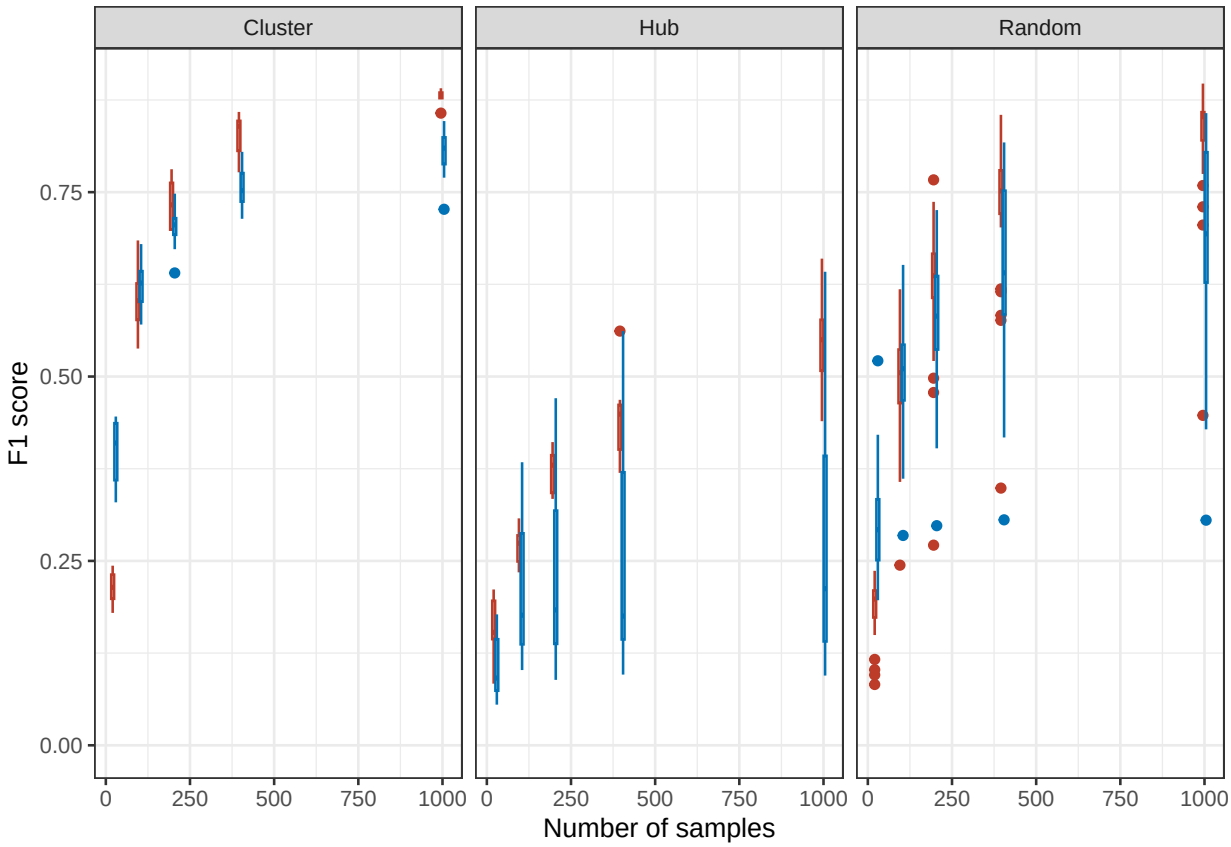

(a) Multivariate normal data

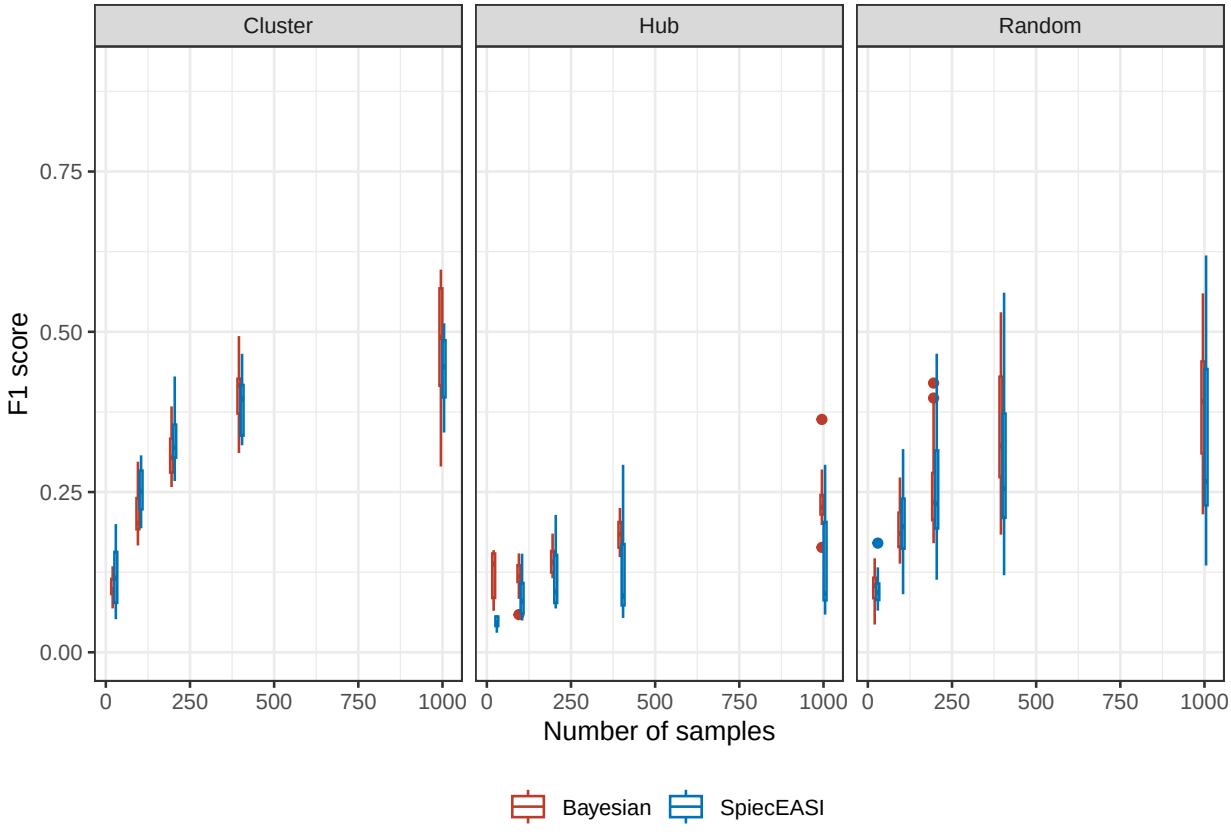

(b) CLR -transformed microbial counts

Figure 3: Recovery depends on sample size, underlying network topology, and data type. We show the F1 score across different data types, sample sizes, and methods. All the networks contained 100 nodes (taxonomic units). A total of 1590 models were evaluated.

whose posterior inclusion probability was greater than 0.5. Both strategies were the default strategies in their respective R libraries.

3.2.1 F1-score

Figure 3 shows the F1-score for different sample sizes and datasets. The F1-score summarizes precision (number of true-positive edges divided by the number of edges) and recall (number of true-positive edges divided by the number of true edges). For both the methods, the inference improved with the sample size. We observed differences among the three topologies, with the most challenging being the hub topology. Linking the data to microbial counts and applying the centered log-ratio transformation afterward adversely affected recovery, which became more weakly dependent on the sample size (see Figure 3b). The inference for a sample size of 25 was poor in all the cases (F1 < 0.25).

The Bayesian method performed significantly better than SpiecEASI with both normal-multivariate data and microbial counts (p = 6.6e-07 and p = 9.4e-09 from a paired-Welch test on the difference of F1 means). SpiecEASI exhibited greater variability than the Bayesian method when considering a fixed graph structure and sample size. A portion of this variability can be attributed to the differences in the maximum degree[9], denoted by d, across various simulated graphs. We found the d term to be significant in a likelihood ratio test (p =1.3e-14) for SpiecEASI but not for the Bayesian method.

3.2.2 Precision versus recall

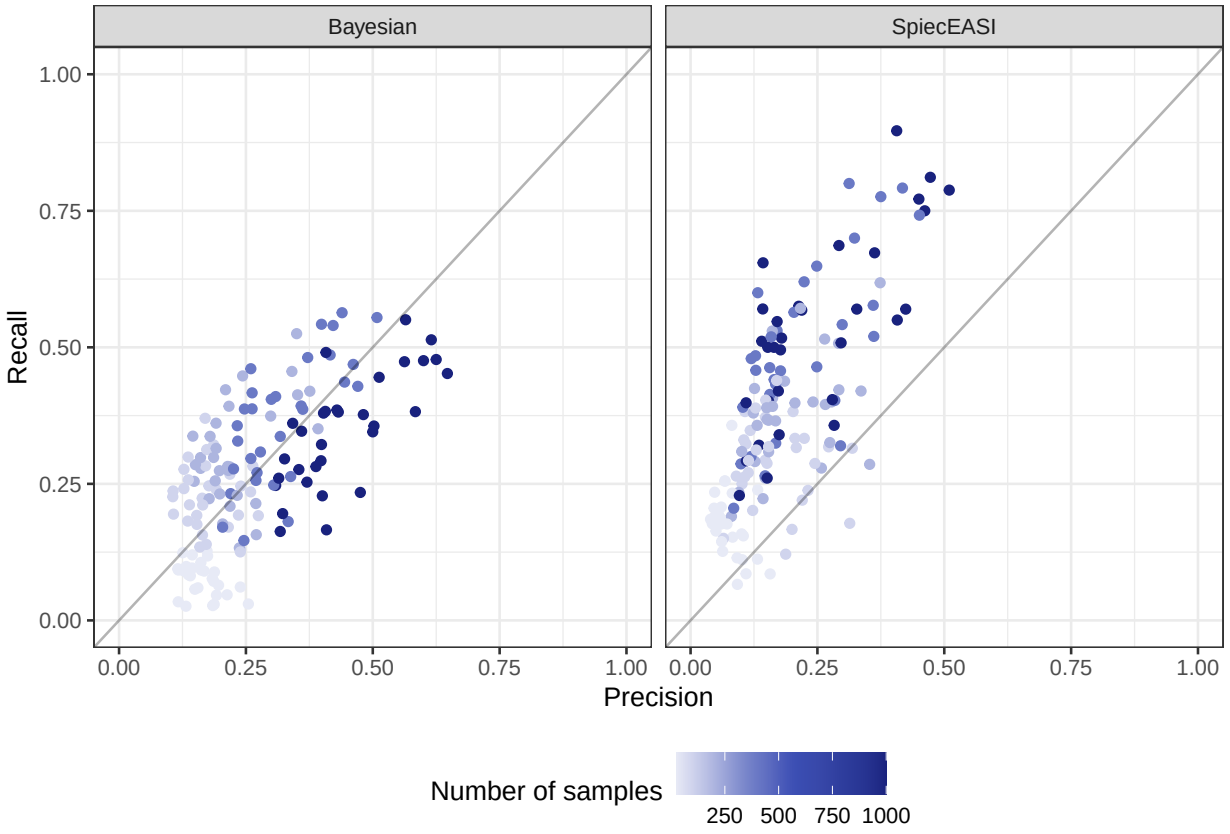

Figure 4: SpiecEASI tended to over-select the edges. We show the recall versus the precision of the same models as Figure 3b (only microbial counts) across different sample sizes.

SpiecEASI tended to overselect edges, so we obtained more complete graphs at the cost of more spurious

[9]The maximum degree is the number of edges of the most connected node in a graph, and it plays an important role in determining the number of samples required to recover the true graph (Kurtz et al. 2015)

edges (see Figure 4). In contrast, the Bayesian method had a more balanced distribution of error types, which was a consequence of the established inclusion threshold $\alpha = 0.5$. With microbial counts, precision was rarely greater than 50% for any of the methods.

3.2.3 k top-ranked edges

We considered the analysis of only the top-ranked edges. We assessed the proportion of incorrect edges when only edges with the highest confidence were considered. We compared both methods by including the k top-ranked edges (see Figure 5) according to their inclusion probability (Bayesian method) or their stability between resamples (SpiecEASI).

The success of this strategy was highly dependent on sample size. However, it provided better results for the SpiecEASI, especially for small samples. Our results suggest that obtaining relatively high precision (above 50%) might be feasible if we restrict our analysis to the k-top ranked edges. We discuss the difficulty of choosing k later.

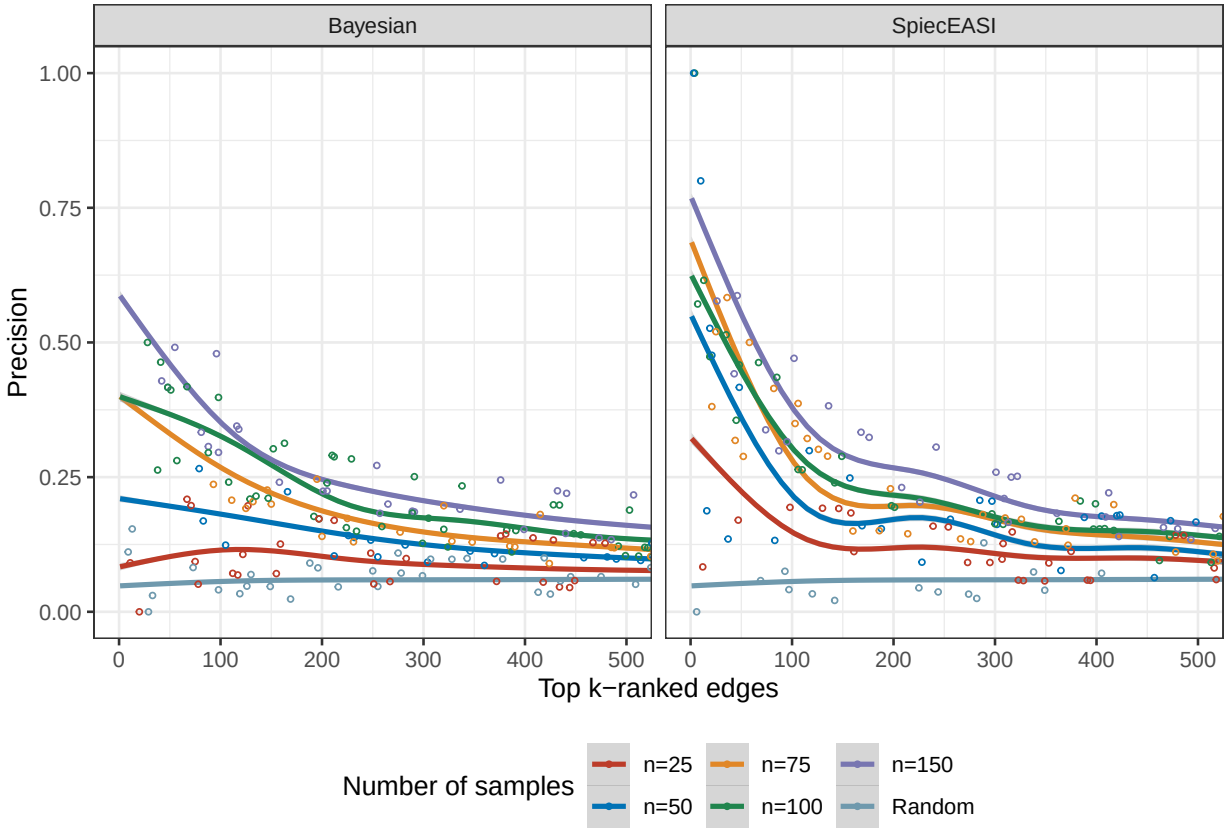

Figure 5: Selecting the k top-ranked edges of SpiecEASI improved the accuracy for small sample sizes. We show precision when predicting only the presence of the top k-ranked edges. We ranked the edges according to the probability of inclusion (Bayesian) and the stability between resamples (SpiecEASI). Different lines show the tendencies across sample sizes. We included randomly sampled points from the dataset for better visualization. We evaluated the expected precision when selecting edges randomly (gray baseline).

3.3 Predicting network properties

We analyzed the error of three representative metrics across increasing sample sample sizes: modularity, hub score, and distances between taxonomic units. The Bayesian method performed better on the three metrics and it was more robust to variations in true networks than the SpiecEASI method. This result was consistent across topologies, graph sizes, and dataset types (normal multivariate or microbial counts).

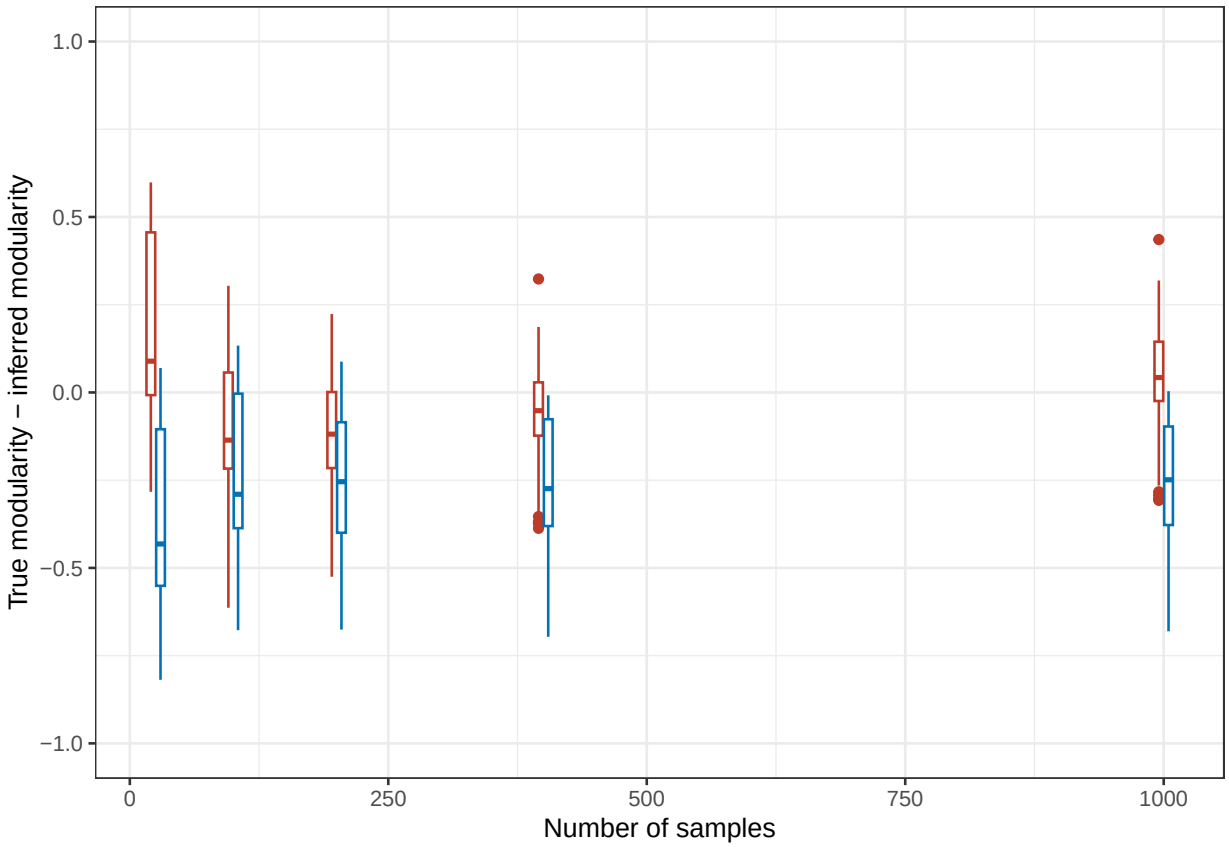

(a)

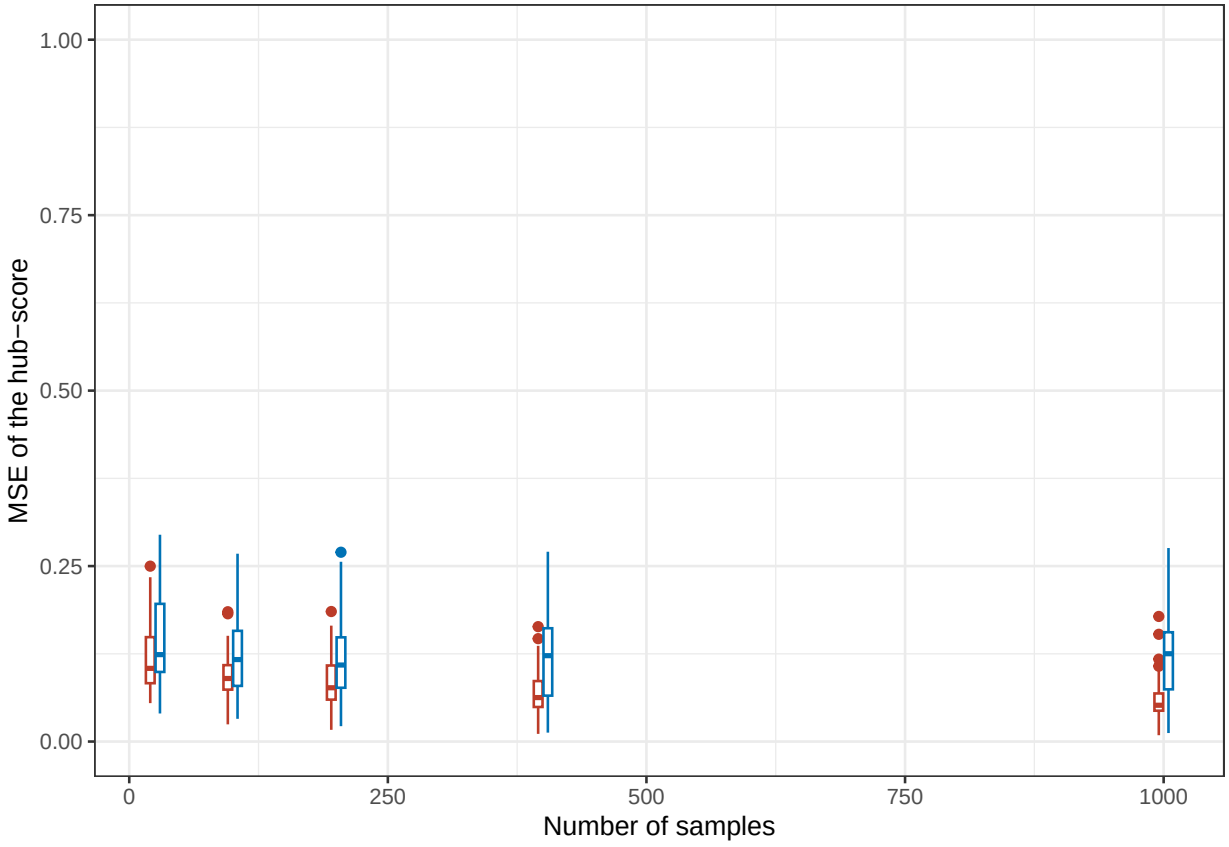

(b)

Figure 6: The predicted network properties may be unreliable, especially for low sample sizes. We show the results for the same models as Figure 3b (microbial counts only). (a) Differences between the true and predicted modularities. (b) Mean square error (MSE) of each node's true and predicted hub scores.

Regarding modularity, the error was considerably high, especially at low sample size, for both methods (see Figure 6a). SpiecEASI systematically overestimated modularity. The mean square error (MSE) of the hub scores was relatively low, below 30% even when $n < p$ (see Figure 6b). The distances between nodes were the least reliable metrics. Unlike the modularity and hub score, which did not improve substantially, the sample size affected the correlation between the true and inferred distances greatly. For low sample size, $n < p$, the Spearman correlation was systematically poor (close to zero).

3.4 Module identification

We evaluated the reliability of modules of taxonomic units co-occurring together. We clustered the networks after excluding edges that corresponded to negative correlations using the Walktrap algorithm (Pons and Latapy 2005). We compared the true and inferred clusters using the adjusted mutual information (AMI). The AMI metric compares the similarity between two partitions of potentially different sizes, and takes a value of one if both partitions are identical and zero when the overlap equals the expected by chance alone (Vinh, Epps, and Bailey 2009).

The obtained clusters were surprisingly reliable, and SpiecEASI (not using the Meinshausen and Bühlmann method, but estimating the whole precision matrix) was consistently better than the Bayesian alternative (see Figure 7). Even for a middle sample size, meaningful clusters can be obtained.

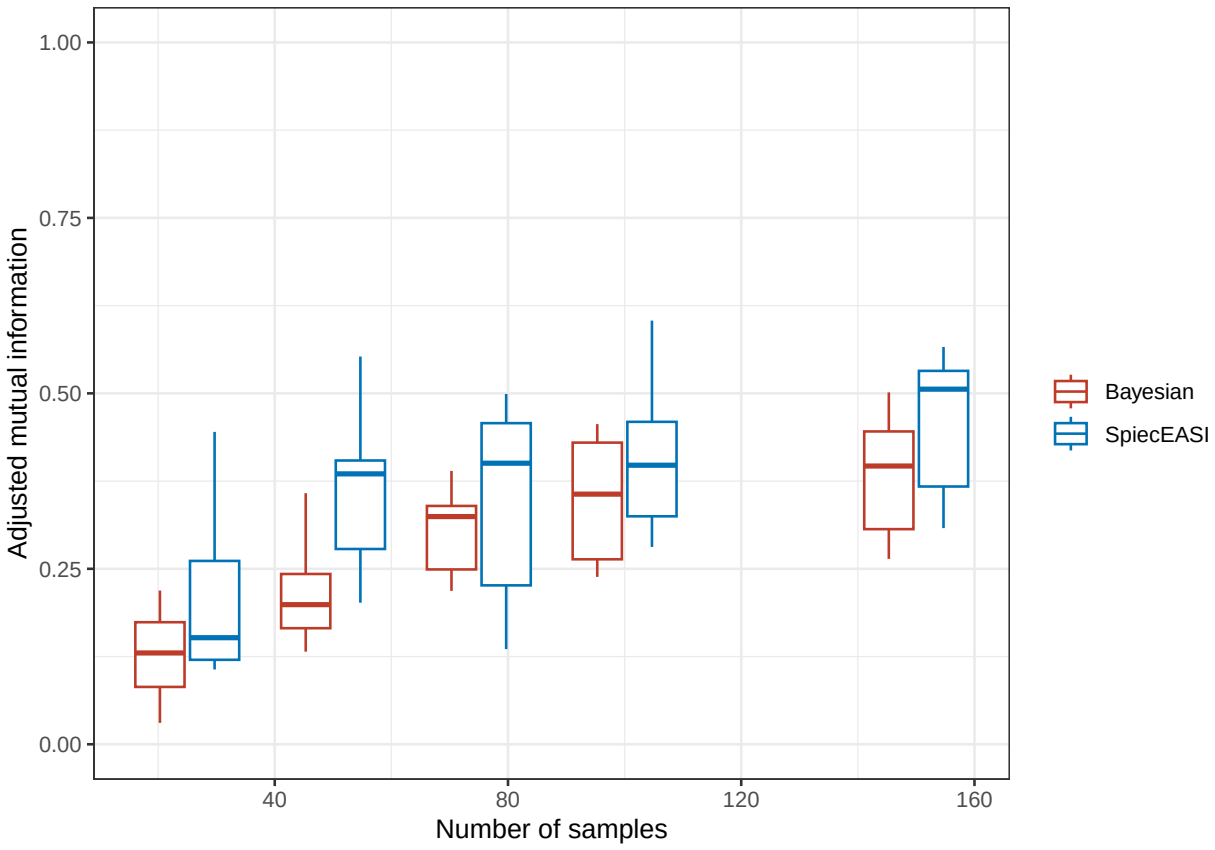

Figure 7: SpiecEASI provides more reliable cluster partitions. We show the adjusted mutual information between the true and predicted clusters for five networks across different sample sizes. Clusters were obtained only by considering positive correlations between taxonomic units.

3.5 Confidence and credibility intervals

Finally, we computed bootstrapping confidence intervals for SpiecEASI and credibility intervals for the Bayesian method. We did it for all previous metrics except for module identification. To our knowledge, the

BDgraph implementation does not provide posterior samples of the precision matrix, so we did not compute any credibility intervals involving the sign of the edges.

We show the results only of the hub score estimated from microbial, as it is the one we analyzed in more detail (see Figure 8b). We chose this metric because it is the most well-known. Similar results were obtained for the other measures when estimating microbial counts. The 95% confidence intervals were wide, as their range was between 25% and 75% of the entire range of possible values (from zero to one). The fraction of nodes whose credibility or confidence interval contains their true hub score oscillates within the same range.

There is a negative relationship between the number of samples and the bootstrap confidence interval range for SpiecEASI. The fraction of nodes with their true hub score within their 95% confidence interval decreases similarly when the sample size is increased (i.e., increasing the sample size narrows the confidence interval but not around the true value).

The Bayesian model showed a very narrow confidence interval for a small sample size (as it tends to predict sparse networks). For larger sample sizes, a very weak negative correlation was observed. We saw no big improvements for the Bayesian method when increasing the sample size, as the fraction of nodes' hub scores within their 95% credibility interval oscillated around 25% and 75%.

4 Methods

All the scripts used in this project can be found in github.com/currocam/microbial-network-inference. All statistical analysis was done in R (R Core Team 2021).

4.1 Simulation of synthetic datasets

Random networks were simulated by assigning a Bernoulli random variable, where p was fixed for every network and drawn from a uniform distribution between 0.01 and 0.1. The hub networks were simulated by assigning each node to a random g group. Each group is then assigned a center (from itself) and one edge is inserted for every node with its center. The number of hubs g was randomly chosen as an integer from one to ten. The cluster networks were simulated by assigning each node to a random g group (sampled from 1 to 10). We then assigned a Bernoulli random variable with $p = 0.2$ between every pair of nodes belonging to the same group.

We used BDgraph to simulate data from a negative binomial distribution such that its correlations were consistent with the simulated graphs (R. Mohammadi and Wit 2019). We simulated unequal depth sequencing by multiplying by a correction factor (sampled from a uniform distribution [0.75, 1.25]).

4.2 Fitting graphical models with SpiecEASI

We fitted graphical models using the Pulsar implementation (Müller, Bonneau, and Kurtz 2016), as described by Kurtz et al. (2015). A single-threaded Julia implementation was also made and it is available in the repository (github.com/currocam/microbial-network-inference/blob/main/src/StARS_MB.jl).

4.3 Fitting graphical models with BDgraph

We used the birth-death MCMC algorithm (R. Mohammadi and Wit 2019), with 10000 iterations, 5000 burn-in iterations and a single chain. We assigned an uninformative prior to the graph space (all graphs are equally plausible) but set the initial graph to be empty. The chosen G-Wishart prior distribution has two degrees. We assessed the convergence by tracing the graph size across the chain.

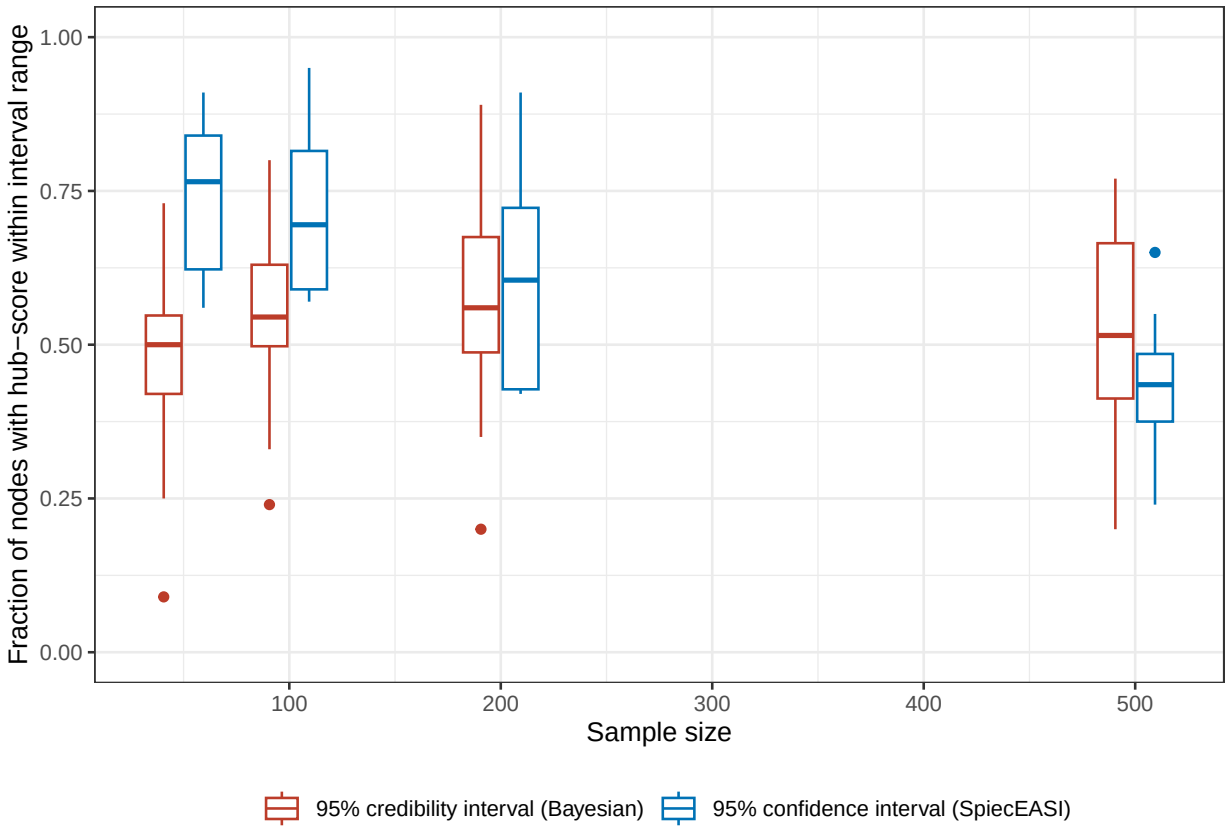

(a) Fraction of nodes with hub-score within the 95% credibility or confidence interval

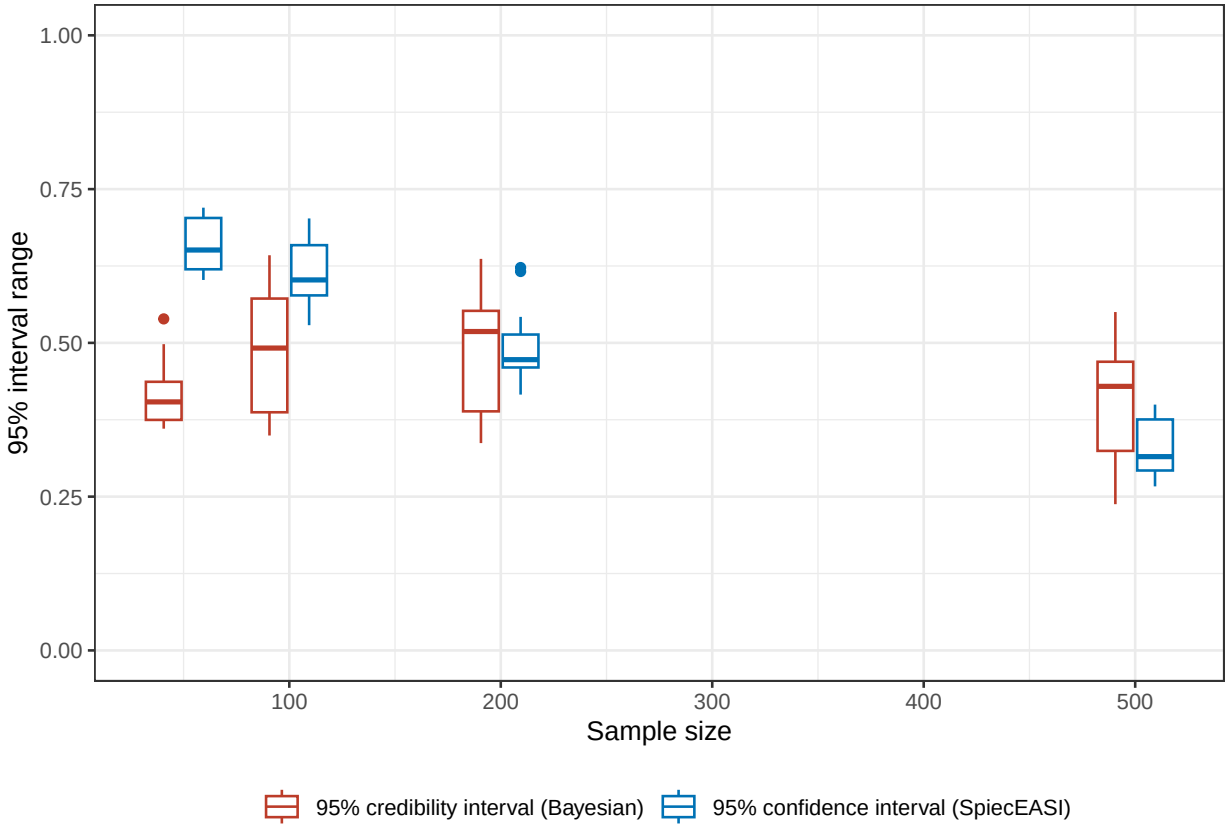

(b) 95% credibility or confidence interval range

Figure 8: The use of credibility or confidence intervals is unlikely to increase statistical robustness. We show the results for ten random networks estimated from microbial counts with low sample sizes. (a) Fraction of nodes whose true values are within the 95% credibility or 95% confidence interval. (b) Range of each interval (i.e., $Q_{0.975} - Q_{0.025}$).

4.4 Recovery of microbial networks

We assessed the recovery of both methods by comparing the adjacency matrix of the true and inferred graph. The likelihood ratio test was conducted using the lmtest R package (Zeileis and Hothorn 2002). The specified full and reduced model were F1 $\sim$ sample size+maximum degree+topology and F1 $\sim$ sample size+topology, respectively.

4.5 Network properties

All network properties were computed using the igraph implementation (Csardi and Nepusz 2006). We computed modularities according to the community structure we found using the Walktrap algorithm (Pons and Latapy 2005). We computed Kleinberg's hub score and scaled it so one is the maximum score (Kleinberg 1998b).

4.6 Module identification

We excluded edges that did not correspond to positively correlated taxonomic units by excluding edges such that $\Omega_{i,j} > 0$. We used either the posterior estimation of the precision matrix (Bayesian) or the precision matrix estimated according to Friedman, Hastie, and Tibshirani (2008) with StARS optimal λ (SpiecEASI). We identified the modules using the Walktrap algorithm (Pons and Latapy 2005) and then computed the AMI metric as implemented in the aricode R package (Vinh, Epps, and Bailey 2009).

4.7 Credibility and confidence intervals

We computed the confidence intervals by performing 100 bootstraps and the credibility interval by drawing 5000 samples from the posterior. The network properties were then computed as mentioned before.

5 Discussion

5.1 Simulation of synthetic datasets

There is no standard protocol for the simulation of synthetic datasets for network construction (Matchado et al. 2021), and there is a need for theoretical justification for the many choices that must be made. For example, we do not know which network topologies are representative of true networks. Although simulating random networks is the obvious choice in the absence of more information, we still have to decide how sparse the network to be (ex., if we model the absence/presence of every edge as a Bernoulli random variable, we still have to decide which probability to use). We chose to simulate a wide range of graph sizes. This range is, however, arbitrary and hard to justify.

All methods, whether explicitly or implicitly, assume a latent normal multivariate random variable is somehow linked to the microbial abundances. We constructed the synthetic datasets by first simulating the latent variable and then simulating the counts according to a negative binomial in such a way the abundances were correlated in the same way as in the original latent variable. We decided to do so because this approach was already implemented in SpiecEASI and BDgraph (both R packages we used to infer the networks) (Kurtz et al. 2015; R. Mohammadi and Wit 2019). However, a better option would have been to explicitly model the relationship between both variables, as it would be a more transparent process.

5.2 Recovery of microbial networks

Published methods are challenging to compare because their articles report results under different conditions (i.e., sample size, number of taxonomic units, sparsity of true graphs, or generative models) (Kurtz et al.

2015; Jiang et al. 2020; Vinciotti, Behrouzi, and Mohammadi 2022). In addition, the authors emphasized favorable settings with high sample sizes and relatively few taxonomic units, which might be unfeasible in typical microbiology-ecology projects.

We evaluated the recovery under what I argue are more realistic settings. The analysis is, however, limited to a few network topologies, sample sizes, graph sizes, and a fixed number of taxonomic units. Then, our conclusions are limited and should be considered cautiously. We opted to replicate our results across different random seeds rather than explore a larger space of parameters. It would be interesting to replicate our experiments in wider conditions.

5.2.1 F1-score

Recovering the whole true microbial network is an unrealistic goal. This has already been recognized by others (Kurtz et al. 2015). The F1 score was very low for the microbial counts datasets (see Figure 3b), but it was also low for those we inferred directly from the normal multivariate data (see Figure 3a). I argue that it is unreasonable to expect the method to perform better when providing as input something else rather than what it would correspond to the latent variable. If that is the case, this result would be independent of how we simulate the counts or the transformation of choice (centered log ratio, in our case).

In addition, our results suggest that the graph size (that correlates with the maximum degree) and the underlying true topology impacts the recovery. It is difficult to establish how relevant it is in the absence of information on how dense and what topology the networks we are trying to model have. However, our Bayesian alternative was much less affected, so this is a positive point in its favor against SpiecEASI.

5.2.2 Precision versus recall

Researchers should carefully consider how the number of missing and spurious edges would impact their analysis. SpiecEASI is based on StARS, a selection method that was designed to overestimate the number of edges. We found exactly the expected trend (see Figure 4).

Despite SpiecEASI being widely used, it is not common practice to justify whether that choice is appropriate. Favoring one type of error, at the expense of the other, is not pertinent in all cases. In that sense, the Bayesian alternative could be tuned for the specific research questions by choosing a different threshold α. The predicted graph includes all edges for which the posterior probability is greater than α. Decreasing α favors recall, and increasing it favors precision.

5.2.3 k top-ranked edges

We confirmed Kurtz et al. (2015) results and observed that the precision of SpiecEASI greatly improved when considering only a few top edges (see Figure 5). We did not observe this improvement with the Bayesian method. This is relevant when the researchers do not want to analyze the entire graph, but may want to study the presence of specific edges. For example, counting the number of edges between different taxonomic groups (Hu et al. 2021).

Because the StARS confidence scores do not have a straightforward interpretation, the choice is usually made based on the ranked edges (i.e., choose the k edges we are more confident about). There is no straightforward procedure to choose k, and it is a decision that can lead to artificially statistical results. The same can be sayed from tuning the inclusion threshold of the Bayesian method.

5.3 Predicting network properties

It has been pointed out that recovering the entire microbial network may be unrealistic, and our results suggest the same. However, under certain conditions, inferred networks with errors may reflect the properties

of the true network (Kurtz et al. 2015). Our results, however, are not encouraging.

We analyzed the modularity, the hub score, and the distance between nodes as they are between the most commonly used metrics (Morueta-Holme et al. 2016; Lurgi et al. 2019; Zamkovaya et al. 2021). The three metrics had considerable errors in the studied range of sample sizes. I argue this is a relevant result, as authors might have used very optimistic settings when reporting the errors of the network properties of their methods.

Kurtz et al. (2015) in the original SpiecEASI publication reported the performance of their method when estimating different network properties for the case $n \gg p$, for example n = 1360 samples and p = 205 taxonomic units. This is clearly not the usual case. For example, Doane et al. (2023) estimated different metrics, including modularity, from different networks that had between 100 and 160 taxonomic units (they aggregated at family level) but only between 14 and 19 samples. Our results suggest that researchers should consider that the predicted network properties are error-prone and analyze the implication in their analysis.

Moreover, there is an essential aspect we have deliberately ignored: what happens when we agglomerate several nodes. This can happen intentionally when we agglomerate taxonomic units at a certain level or unintentionally if we fail to distinguish between two species when clustering sequences into taxonomic units. Future work should analyze this aspect, as it is likely another source of errors (Röttjers and Faust 2018).

5.4 Module identification

Module identification is one of the main applications of co-occurrence microbial networks. For this application, SpiecEASI is the obvious winner. First, because it produced a more reliable cluster than the Bayesian method. But also because estimands that involve those modules can easily be bootstrapped in order to get a measurement of uncertainty. As mentioned above, the BDgraph implementation does not provide posterior samples of the precision matrix, which we need if we want to take into account the sign of the edges when calculating credibility intervals. Future work could further optimize the implementation to make this type of application feasible.

When using SpiecEASI, we chose to use the Meinshausen and Bühlmann method instead of estimating the entire matrix because the literature indicated that, although it does not directly provide the sign of the edge, it performs better in terms of speed, recall and precision. Interestingly, we found that SpiecEASI outperformed the Bayesian method only in the single application where we did not use the Meinshausen and Bühlmann method. Would it be worthwhile to analyze whether it is not the optimal choice when estimating network properties?

5.5 Confidence and credibility intervals

Finally, we analyzed to what extent is possible to measure the uncertainty of the metrics using confidence and credibility intervals. Studies that use network properties would benefit from uncertainty measurements. This is especially true given that our results suggest these metrics are often unreliable, especially for low sample sizes.

We focused on the hub-score. We found that the sample size considerably affected both credibility and confidence intervals. Both types of intervals reflected the uncertainty of the method in the sense that they were very wide (from 0.25 to 0.75, which means it ranges from almost half of the domain of possible values). However, the fraction of intervals that did not contain its true value was considerably high (if you take into account the range). Our results suggest that, for low sample sizes, computing confidence or credibility intervals can hardly improve the robustness of the microbial network analysis.

6 Future work

Researchers should not only justify the link between their network estimand and biology, but also consider to what extent they might be reaching the wrong conclusion because of the associated error. This analysis should involve extensive simulation for the specific scientific question and estimand. Moreover, factors such as the impact of merging nodes, even if deliberately during preprocessing, should be taken into account. I argue there is a lack of powerful yet accessible statistical software for this purpose.

Finally, there is a major issue regarding the interpretation of the networks in the absence of environmental factors. Network edges should not be interpreted as interactions, although detection of associations is a valuable intermediate step (Guseva et al. 2022). In the absence of environmental factors (and any confounding variable), the associations might be misleading. Future work should focus on more sophisticated tools that allow the researcher to include those environmental factors, as well as to incorporate biological knowledge (Yoon, Gaynanova, and Müller 2019; Shen and Solis-Lemus 2022).

7 Conclusion

Microbial network inference is a very novel field with many open questions. Although the number of methods available keep increasing, there is no consensus in how to appropriately benchmark the different methods. In the meantime, studies might have overestimated the reliability of the inferred networks. Researchers should carefully consider the expected variability and error associated with their results via extensive simulation of synthetic datasets.

Advances in sequencing technology have already generated the data, but there is a lack of statistical software capable of inferring ecological networks reliably. However, there is a huge potential of biological insights we can gain from new ways of analyzing the data in microbial ecology that goes beyond descriptive studies.

References

Blanchet, F. Guillaume, Kevin Cazelles, and Dominique Gravel. 2020. "Co-Occurrence Is Not Evidence of Ecological Interactions." Edited by Elizabeth Jeffers. Ecology Letters 23 (7): 1050–63. https://doi.org/10.1111/ele.13525.

Carvalho, C. M., and J. G. Scott. 2009. "Objective Bayesian Model Selection in Gaussian Graphical Models." Biometrika 96 (3): 497–512. https://www.jstor.org/stable/27798844.

Chaffron, Samuel, Hubert Rehrauer, Jakob Pernthaler, and Christian von Mering. 2010. "A global network of coexisting microbes from environmental and whole-genome sequence data." Genome Research 20 (7): 947–59. https://doi.org/10.1101/gr.104521.109.

Clauset, Aaron, M. E. J. Newman, and Cristopher Moore. 2004. "Finding Community Structure in Very Large Networks." Physical Review E 70 (6): 066111. https://doi.org/10.1103/PhysRevE.70.066111.

Csardi, Gabor, and Tamas Nepusz. 2006. "The Igraph Software Package for Complex Network Research." InterJournal Complex Systems: 1695. https://igraph.org.

Doane, Michael P., Michael B. Reed, Jody McKerral, Laís Farias Oliveira Lima, Megan Morris, Asha Z. Goodman, Shaili Johri, et al. 2023. "Emergent Community Architecture Despite Distinct Diversity in the Global Whale Shark (Rhincodon Typus) Epidermal Microbiome." Scientific Reports 13 (1): 12747. https://doi.org/10.1038/s41598-023-39184-5.

Faust, Karoline. 2021. "Open Challenges for Microbial Network Construction and Analysis." The ISME Journal 15 (11): 3111–18. https://doi.org/10.1038/s41396-021-01027-4.

Friedman, J., T. Hastie, and R. Tibshirani. 2008. "Sparse Inverse Covariance Estimation with the Graphical Lasso." Biostatistics 9 (3): 432–41. https://doi.org/10.1093/biostatistics/kxm045.

Guseva, Ksenia, Sean Darcy, Eva Simon, Lauren V. Alteio, Alicia Montesinos-Navarro, and Christina Kaiser. 2022. "From Diversity to Complexity: Microbial Networks in Soils." Soil Biology and Biochemistry 169 (June): 108604. https://doi.org/10.1016/j.soilbio.2022.108604.

Ha, Min Jin, Junghi Kim, Jessica Galloway-Peña, Kim-Anh Do, and Christine B. Peterson. 2020. "Compositional Zero-Inflated Network Estimation for Microbiome Data." BMC Bioinformatics 21 (21): 581. https://doi.org/10.1186/s12859-020-03911-w.

Hu, Sarah K., Erica L. Herrera, Amy R. Smith, Maria G. Pachiadaki, Virginia P. Edgcomb, Sean P. Sylva, Eric W. Chan, Jeffrey S. Seewald, Christopher R. German, and Julie A. Huber. 2021. "Protistan Grazing Impacts Microbial Communities and Carbon Cycling at Deep-Sea Hydrothermal Vents." Proceedings of the National Academy of Sciences 118 (29): e2102674118. https://doi.org/10.1073/pnas.2102674118.

Jiang, Shuang, Guanghua Xiao, Andrew Y. Koh, Yingfei Chen, Bo Yao, Qiwei Li, and Xiaowei Zhan. 2020. "HARMONIES: A Hybrid Approach for Microbiome Networks Inference via Exploiting Sparsity." Frontiers in Genetics 11. https://www.frontiersin.org/articles/10.3389/fgene.2020.00445.

Jones, Beatrix, Carlos Carvalho, Adrian Dobra, Chris Hans, Chris Carter, and Mike West. 2005. "Experiments in Stochastic Computation for High-Dimensional Graphical Models." Statistical Science 20 (4). https://doi.org/10.1214/088342305000000304.

Jongerling, Joran, Sacha Epskamp, and Donald R. Williams. 2023. "Bayesian Uncertainty Estimation for Gaussian Graphical Models and Centrality Indices." Multivariate Behavioral Research 58 (2): 311–39. https://doi.org/10.1080/00273171.2021.1978054.

Kleinberg, Jon M. 1998a. "Authoritative Sources in a Hyperlinked Environment." In, 668677. SODA '98. USA: Society for Industrial; Applied Mathematics.

———. 1998b. "Authoritative Sources in a Hyperlinked Environment." In, 668677. SODA '98. USA: Society for Industrial; Applied Mathematics.

Kurtz, Zachary D., Christian L. Müller, Emily R. Miraldi, Dan R. Littman, Martin J. Blaser, and Richard A. Bonneau. 2015. "Sparse and Compositionally Robust Inference of Microbial Ecological Networks." PLOS Computational Biology 11 (5): e1004226. https://doi.org/10.1371/journal.pcbi.1004226.

Li, Yunfan, Bruce A. Craig, and Anindya Bhadra. 2019. "The Graphical Horseshoe Estimator for Inverse Covariance Matrices." https://doi.org/10.48550/arXiv.1707.06661.

Liu, Han, Kathryn Roeder, and Larry Wasserman. 2010. "Stability Approach to Regularization Selection (StARS) for High Dimensional Graphical Models." https://doi.org/10.48550/arXiv.1006.3316.

Lurgi, Miguel, Torsten Thomas, Bernd Wemheuer, Nicole S. Webster, and Jose M. Montoya. 2019. "Modularity and Predicted Functions of the Global Sponge-Microbiome Network." Nature Communications 10 (1): 992. https://doi.org/10.1038/s41467-019-08925-4.

Matchado, Monica Steffi, Michael Lauber, Sandra Reitmeier, Tim Kacprowski, Jan Baumbach, Dirk Haller, and Markus List. 2021. "Network Analysis Methods for Studying Microbial Communities: A Mini Review." Computational and Structural Biotechnology Journal 19 (January): 2687–98. https://doi.org/10.1016/j.csbj.2021.05.001.

Meinshausen, Nicolai, and Peter Bühlmann. 2006. "High-Dimensional Graphs and Variable Selection with the Lasso." The Annals of Statistics 34 (3): 1436–62. https://doi.org/10.1214/009053606000000281.

Mohammadi, A., and E. C. Wit. 2015. "Bayesian Structure Learning in Sparse Gaussian Graphical Models." Bayesian Analysis 10 (1): 109–38. https://doi.org/10.1214/14-BA889.

Mohammadi, Reza, and Ernst C. Wit. 2019. "BDgraph: An R Package for Bayesian Structure Learning in Graphical Models." Journal of Statistical Software 89 (May): 1–30. https://doi.org/10.18637/jss.v089.i03.

Morueta-Holme, Naia, Benjamin Blonder, Brody Sandel, Brian J. McGill, Robert K. Peet, Jeffrey E. Ott, Cyrille Violle, Brian J. Enquist, Peter M. Jørgensen, and Jens-Christian Svenning. 2016. "A Network Approach for Inferring Species Associations from Co-Occurrence Data." Ecography 39 (12): 1139–50. https://doi.org/https://doi.org/10.1111/ecog.01892.

Müller, Christian L., Richard Bonneau, and Zachary Kurtz. 2016. "Generalized Stability Approach for Regularized Graphical Models." https://arxiv.org/abs/1605.07072.

Piironen, Juho, and Aki Vehtari. 2017. "Sparsity Information and Regularization in the Horseshoe and Other Shrinkage Priors." Electronic Journal of Statistics 11 (2): 5018–51. https://doi.org/10.1214/17-EJS1337SI.

Pons, Pascal, and Matthieu Latapy. 2005. "Computing Communities in Large Networks Using Random Walks (Long Version)." https://arxiv.org/abs/physics/0512106.

Power, Mary E., David Tilman, James A. Estes, Bruce A. Menge, William J. Bond, L. Scott Mills, Gretchen Daily, Juan Carlos Castilla, Jane Lubchenco, and Robert T. Paine. 1996. "Challenges in the Quest for Keystones: Identifying Keystone Species Is Difficult—but Essential to Understanding How Loss of Species Will Affect Ecosystems." BioScience 46 (8): 609–20. https://doi.org/10.2307/1312990.

Prosser, James I. 2020. "Putting Science Back into Microbial Ecology: A Question of Approach." Philosophical Transactions of the Royal Society B: Biological Sciences 375 (1798): 20190240. https://doi.org/10.1098/rstb.2019.0240.

R Core Team. 2021. R: A Language and Environment for Statistical Computing. Vienna, Austria: R Foundation for Statistical Computing. https://www.R-project.org/.

Richard Li, Zehang, Tyler H. McCormick, and Samuel J. Clark. 2019. "Bayesian Joint Spike-and-Slab Graphical Lasso." Proceedings of Machine Learning Research 97 (June): 3877–85. https://www.ncbi.nlm.nih.gov/pmc/articles/PMC7845917/.

Röttjers, Lisa, and Karoline Faust. 2018. "From Hairballs to Hypotheses–biological Insights from Microbial Networks." FEMS Microbiology Reviews 42 (6): 761–80. https://doi.org/10.1093/femsre/fuy030.

Roverato, Alberto. 2002. "Hyper Inverse Wishart Distribution for Non-Decomposable Graphs and Its Application to Bayesian Inference for Gaussian Graphical Models." Scandinavian Journal of Statistics 29 (3): 391–411. https://www.jstor.org/stable/4616723.

Shen, Yunyi, and Claudia Solis-Lemus. 2022. "Bayesian Chain Graph LASSO Models to Learn Sparse

Microbial Networks with Predictors." https://arxiv.org/abs/2012.08397.

Uhler, Caroline. 2017. "Gaussian Graphical Models: An Algebraic and Geometric Perspective." https://doi.org/10.48550/arXiv.1707.04345.

Vinciotti, Veronica, Pariya Behrouzi, and Reza Mohammadi. 2022. "Bayesian Inference of Microbiota Systems from Count Metagenomic Data." https://arxiv.org/abs/2203.10118.

Vinh, Nguyen Xuan, Julien Epps, and James Bailey. 2009. "Information Theoretic Measures for Clusterings Comparison: Is a Correction for Chance Necessary?" In, 10731080. ICML '09. New York, NY, USA: Association for Computing Machinery. https://doi.org/10.1145/1553374.1553511.

Wang, Hao. 2012. "Bayesian Graphical Lasso Models and Efficient Posterior Computation." Bayesian Analysis 7 (4). https://doi.org/10.1214/12-BA729.

Yoon, Grace, Irina Gaynanova, and Christian L. Müller. 2019. "Microbial Networks in SPRING - Semi-Parametric Rank-Based Correlation and Partial Correlation Estimation for Quantitative Microbiome Data." Frontiers in Genetics 10. https://www.frontiersin.org/articles/10.3389/fgene.2019.00516.

Zamkovaya, Tatyana, Jamie S. Foster, Valérie de Crécy-Lagard, and Ana Conesa. 2021. "A Network Approach to Elucidate and Prioritize Microbial Dark Matter in Microbial Communities." The ISME Journal 15 (1): 228–44. https://doi.org/10.1038/s41396-020-00777-x.

Zeileis, Achim, and Torsten Hothorn. 2002. "Diagnostic Checking in Regression Relationships." R News 2 (3): 7–10. https://CRAN.R-project.org/doc/Rnews/.